

See discussions, stats, and author profiles for this publication at: <https://www.researchgate.net/publication/231671007>

Characterization of Protein Adsorption and Immunosorption Kinetics in Photoablated Polymer Microchannels

ARTICLE *in* LANGMUIR · OCTOBER 2000

Impact Factor: 4.46 · DOI: 10.1021/la0006667 · Source: OAI

CITATIONS

57

READS

59

5 AUTHORS, INCLUDING:



Girdharan Gokulrangan

Pfizer Inc.

19 PUBLICATIONS 524 CITATIONS

SEE PROFILE



Hubert H Girault

École Polytechnique Fédérale de Lausanne

559 PUBLICATIONS 14,028 CITATIONS

SEE PROFILE



George S Wilson

University of Kansas

212 PUBLICATIONS 9,274 CITATIONS

SEE PROFILE

Characterization of Protein Adsorption and Immunosorption Kinetics in Photoablated Polymer Microchannels

Joël S. Rossier,[†] Giridharan Gokulrangan,[‡] Hubert H. Girault,^{*,†}
Stanislav Svojanovsky,[‡] and George S. Wilson[‡]

Laboratoire d'Electrochimie, Ecole Polytechnique Fédérale de Lausanne, CH-1015 Lausanne, Switzerland, and Department of Chemistry, University of Kansas, Malott Hall, Lawrence, Kansas, KS-66045

Received May 12, 2000. In Final Form: July 31, 2000

A preliminary characterization of protein adsorption and immunosorption kinetics carried out in polymer microchannels is reported. A photoablated poly(ethylene terephthalate) (PET) surface and a PET/polyethylene sealing laminate were used for the channel microfabrication. The surface state of the PET channel substrate and PET/polyethylene lamination were analyzed by using SEM and ATR-FTIR spectroscopy techniques. Protein adsorption and immunosorption studies were carried out using staphylococcal enterotoxin B (SEB) and polyclonal anti-SEB antibody (Ab) samples. Affinity purified polyclonal rabbit (Rb) anti-SEB Ab was radioiodinated and adsorbed in the microchannel. It was determined that the maximum amount of adsorbed antibody was about 13.0 pmol·cm⁻² (about 2 μg·cm⁻²), which corresponds to 0.81 pmol per microchannel. The distribution of the adsorbed protein on the walls of the microchannel depended on the surface state of the polymer exposed to the solution. The amount of the radiolabeled antibody adsorbed on the photoablated PET was about 19.4 pmol·cm⁻², whereas it was only 5.5 pmol·cm⁻² on the PET/polyethylene lamination. About 30% of the anti-SEB Ab adsorbed on the microchannel surface was found to be biologically active. A study of the kinetics of the SEB–anti-SEB Ab immunochemical reaction was also carried out. It could be substantiated that the forward reaction is diffusion controlled and that the equilibrium for such a reaction could be achieved within about 1 min in the microchannels. This is in good agreement with the calculation of a diffusion-controlled reaction in such a microchannel, according to Fick's second law.

Introduction

The principal objective of this work is to demonstrate the utility of polymer microchannel-based analysis systems in carrying out rapid immunochemical reactions. Apart from the typical merits of such miniaturized systems such as limited reagent consumption and faster analysis time, the use of a microchannel-based system yields an enhanced surface-to-volume ratio and increased mass transport efficiency due to its very small dimensions. Standard immunosorbent assays often require incubation times of several hours when the reaction is carried out in microtiter plates. The intrinsic rate of the antigen–antibody reaction in solution is high,¹ but it can be demonstrated that the time required for the reaction to reach completion on surfaces is often related to the mass transport efficiency of the molecules to the immunosorbent surface. Several strategies have been adopted to speed up this process. Beads in the 1–3 μm diameter range are frequently used, as they provide an advantageous surface-to-volume ratio and also can be conveniently renewed.^{2,3} Elevation of temperature^{4–6} is sometimes applied, but this

does not provide a significant increase in the overall mass transport efficiency. Another approach is to minimize the diffusion distances by decreasing the size of the reactors. The technique, presented as a capillary immunoassay,⁷ utilized capillaries (530 μm i.d) to carry out immunochemical reactions. However, even such dimensions are too large for carrying out rapid immunoassays. Also, the detection was made outside the capillary, thereby rendering the assay difficult to implement in parallel.

The development of microfluidic devices has opened the possibility of using microchannel arrays for electroosmotically driven immunoassay^{8,9} or for electrochromatography¹⁰ with high application potential. Polymer microfluidic devices⁹ were also developed with the inclusion of microelectrodes¹¹ and micropatterning of proteins.^{12,13} Such systems can also be used in the development of an enzyme-linked immunosorbent assay (ELISA) system where the incubation times are reduced and the detection is done in the microdevice itself.¹⁴

The present work shows preliminary results of protein adsorption and immunosorption kinetics in a photoablated

[†] Ecole Polytechnique Fédérale de Lausanne.

[‡] University of Kansas.

(1) Steward, M. W. In *Handbook of experimental immunology*; Wier, D. M., Ed.; Blackwell: Oxford, 1986; Vol. 1, pp 25.1–25.30.

(2) Locascio-Brown, L.; Martynova, L.; Christensen, R. G.; Horvai, G. *Anal. Chem.* **1996**, *68*, 1665–1670.

(3) Willumsen, B.; Christian, G. D.; Ruzicka, J. *Anal. Chem.* **1997**, *69*, 3482–3489.

(4) Butler, J. F. *Immunochemistry of solid-phase immunoassay*; CRC Press: Boca Raton, FL, 1991.

(5) Beumer, T.; Timmerman, B. *Anal. Chem.* **1997**, *69*, 5182–5185.

(6) Beumer, T.; Haarbosch, P.; Carpay, W. *Anal. Chem.* **1996**, *68*, 1375–1380.

(7) Jiang, T.; Halsall, H. B.; Heineman, W. R. *J. Agric. Food Chem.* **1995**, *43*, 1098–1104.

(8) Chiem, N.; Harrison, D. J. *Anal. Chem.* **1997**, *69*, 373–378.

(9) Chiem, N. H.; Harrison, D. J. *Clin. Chem.* **1998**, *44*, 591–598.

(10) Kutter, J. P.; Jacobson, S. C.; Matsubara, N.; Ramsey, J. M. *Anal. Chem.* **1998**, *70*, 3291–3297.

(11) Rossier, J. S.; Roberts, M. A.; Ferrigno, R.; Girault, H. H. *Anal. Chem.* **1999**, *71*, 4294–4299.

(12) Martin, B. D.; Gaber, B. P.; Patterson, C. H.; Turner, D. C. *Langmuir* **1998**, *14*, 3971–3975.

(13) Schwarz, A.; Rossier, J. S.; Roberts, M. A.; Girault, H. H.; Roulet, E.; Mermod, H. *Langmuir* **1998**, *14*, 5526–5531.

(14) Rossier, J. S.; Reymond, F.; Girault, H. H. Patent Application GB 9907249.8, JY & GW Johnson, 1999.

polymer microchannel with radiometric detection. The protein used for this study is staphylococcal enterotoxin B (SEB),¹⁵ because of the wide interest in the rapid detection of this 29 kDa protein.¹⁶ Actually SEB is a frequent trigger of food poisoning, causing gastric disorder when ingested, and can even be lethal.¹⁷ Due to its remarkable stability and toxicity, SEB is considered a prime threat as a biological warfare agent.

Material and Methods

UV Laser Microfabrication. The microfabrication of the channel was performed by UV laser photoablation. This technique, developed for manufacturing microfluidic devices, has been fully described in several recent reports.^{19,20} Briefly, the water-rinsed poly(ethylene terephthalate) (PET) substrate is laminated on one side with a protecting layer made up of PET/polyethylene at 125 °C and 2 bar pressure with an industrial lamination apparatus (Morane, U.K.). The PET substrate is then mounted on a XY stage (Microcontrol, France) and exposed to a mask patterned 193 nm beam from an ArF Excimer laser generating 23 ns pulses (power 10 MW) at a frequency of 50 Hz. The substrate is then moved in the XY plane so that the speed of the displacement and the repetition rate of the laser define a 40 μm deep cavity. Special attention has been given to the design of the inlet and outlet apertures in contact with the microchannel (Figure 1a). The $1 \times 0.1 \text{ mm}^2$ apertures were made by laser drilling of microholes all the way through the PET substrate and the protective laminate. The channel structure with microholes at each end is then sealed with the PET/polyethylene lamination. The channels are $40 \times 100 \mu\text{m}^2$ in cross section and 2 cm long. The surface dimensions of the channel (0.062 cm^2) are slightly larger than what is expected from simple calculation from a $40 \times 100 \mu\text{m}^2$ microchannel due to the shape of the exit that is made of a $1 \text{ mm} \times 40 \mu\text{m}$ rectangular opening at both ends of the microchannel. The choice of the polymer is motivated by the favorable physicochemical properties which the photoablated PET material offers (enhanced surface-to-volume ratio, ability to generate electroosmotic flow, and the easy introduction of microelectrodes) toward realizing our long-term goals of designing micrototal analysis systems.

Spectroscopic Characterization. The surface state of the PET/polyethylene lamination and the photoablated PET have been characterized by scanning electron microscopy (SEM, JEOL 6300 F, USA) before and after the laser treatment. The lamination surface, which forms the top of the microstructure, was studied by attenuated total internal reflection Fourier transformed infrared spectroscopy (ATR-FTIR) with a diamond Golden Gate apparatus (Perkin-Elmer, USA).

Radiolabeling Procedure. Staphylococcal enterotoxin B (SEB), isolated from strains of gram positive cocci *Staphylococcus aureus*, was obtained from Sigma Immunochemicals, MO. Rabbit anti-SEB antibody (Rb anti-SEB Ab) was also obtained from Sigma. Further purification of the antiserum sample was done using affinity chromatography on a Reactigel 6X (Pierce Chemicals, IL) column. SEB was immobilized according to the manufacturer's protocol on the 50 μm particle size column matrix, which is 6% cross-linked agarose. The polyclonal antiserum sample was passed through a 0.5 mL column matrix containing immobilized SEB at a flow rate of 0.5 mL/min. Multiple washings of the column were done with Tris buffer (0.01 M, pH 7.4) to remove weakly bound antibody. The strongly held anti-SEB Ab was further eluted out using immunopure gentle Ag/Ab elution buffer (Pierce). The radioiodination of the affinity purified antibody was performed following the procedure proposed by Markwell.²¹ The Iodobead reagent (Pierce) was used for the radioiodination, and the labeling reaction was performed as per the recommended protocol. A total of six beads was used for the reaction. The separation of labeled proteins and radioactive free

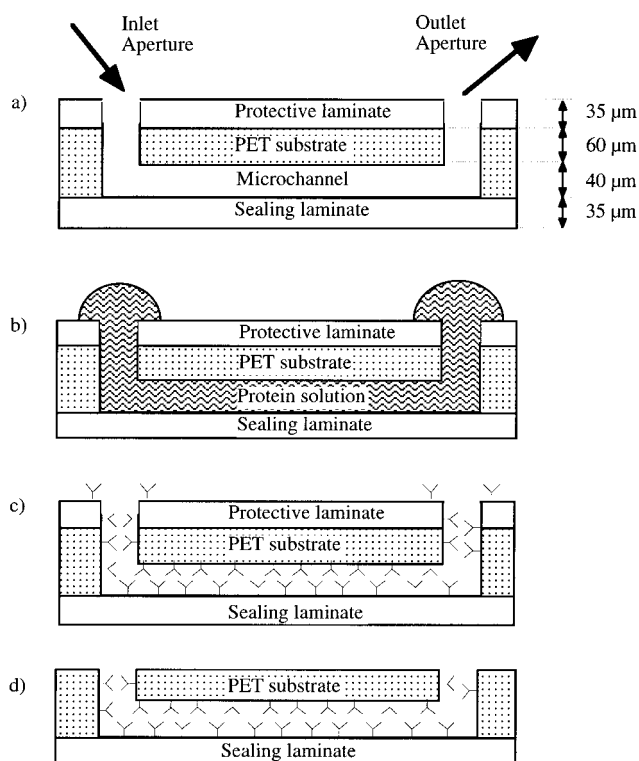


Figure 1. (a) Design and dimensions of the polymer microchannel fabricated by UV laser photoablation of PET and laminated by PE/PET. The structure is composed of a sandwich: protective laminate, PET substrate, and sealing laminate. (b) Schematic of the microfluidics during flow of protein solutions through the photoablated microchannel for adsorption and immunosorption studies. Hemispherical projections near the inlet and outlet apertures indicate the drop size of the protein solution used. Parts c and d indicate the distribution of adsorbed antibodies on the channel surface before and after removal of the protective laminate, respectively. Only the protein adsorbed inside the microchannel is thus effectively measured.

iodine was done using the iodine trap and the Sephadex desalting column supplied along with the carrier free ^{125}I . This step is extremely important because even small amounts of radioactive free iodine remaining entrapped in the radiolabeled proteins may lead to serious errors in the estimation of adsorbed proteins. Reconcentration of the labeled proteins was performed using a preparative ultracentrifuge (Beckman GPR centrifuge, CA) and 2 mL filter tubes (Fisher Scientific, NJ). One milliliter of pure iodinated proteins was obtained, and the final concentration was found to be 2.5 mg/mL using bicinchoninic acid (BCA) protein assay reagent (Pierce). The biological activity of the protein before and after the labeling procedure was determined using the apparent K_i calculated from ELISAs on a polystyrene high-binding microtiterplate (Corning Costar Corporation, NY). The binding was detected using a V_{max} kinetic microplate reader (Molecular Devices, CA) connected to a Windows-based PC.

Protein Adsorption and Immunoassays. The adsorption of the radiolabeled antibody in the microchannel was performed by placing a 8 μL drop of a given protein concentration, from 1 to 2500 $\mu\text{g/mL}$, in coating buffer (0.1 M carbonate buffer, pH 9.5) on top of the inlet aperture (Figure 1b). Most of the solution was then aspirated with a syringe at the outlet aperture. The exact amount of the protein solution in contact with the microchannel was determined using mass balance calculations. The microchannel was then incubated for 1 h at room temperature. The channels were emptied by aspiration between all steps in the assays and washed three times with 10 μL of washing buffer solution (PBS buffer, pH 7.4 with 0.02% Tween 20). It is to be pointed out that the volume of the washing solution is about 100 times that of the channel, which ensures a very efficient washing step. Before γ counting, the protective laminate (Figure 1c and d) is peeled off in order to count only the protein loaded inside the channel and not that around the apertures. The channels

(15) Schantz, E. J.; Roessler, W. J.; Eagman, J.; Spero, L.; Dunnery, D. A.; Bergdoll, M. S. *Biochemistry* **1965**, *6*, 1011–1016.

(16) Rowe, C. A.; Scruggs, S. B.; Feldstein, M. J.; Golden, J. P.; Ligler, F. S. *Anal. Chem.* **1999**, *71*, 433–439.

(17) Hughes, J. M.; Tauxe, R. V. In *Principles and Practice of Infectious Diseases*; Mandell, G. L., Douglas, R. G., Bennet, J. E., Eds.; Churchill Livingstone: New York, 1990.

were then individually counted during 1 min with a γ counter (1282 Compugamma CS, LKB Wallac, 36 MeV). To determine the specific radioactivity of the labeled proteins, a 2 μ L drop of 1.5 mg/mL labeled protein was placed near the inlet aperture and aspirated before incubation and γ counting. It was observed that the calibration for the protein adsorption inside the channels was comparable to that made outside. The radioactivity measurements were always decay corrected when recorded.

The avidity of the pure rabbit (Rb) anti-SEB antibody was checked on a high-binding 96 well microtiter plate before radiolabeling using a titration assay. A uniform concentration, 0.18 μ M, of SEB was adsorbed in the coating buffer solution during an incubation time of 1 h at 37 °C. After washing the plate sufficiently with wash buffer, the unoccupied plate surface was blocked with a blocking buffer, which was a 2% BSA solution in washing buffer. Different concentrations of Rb anti-SEB detection Ab solutions, in molar excess, were then serially added to different wells of the plate followed by 1 h of incubation at 37 °C. Subsequent washing was followed by addition of horseradish peroxidase (HRP)-labeled goat (Gt) anti-Rb reporter Ab for detection of bound SEB. The same procedure was followed for estimating the bioactivity of the radioiodinated antibody.

The bioactivity of the adsorbed antibody in the microchannel was checked with a sandwich assay procedure. Various amounts of nonlabeled Rb anti-SEB Ab, from 0.06 to 0.31 pmol, were adsorbed in different channels following the procedure presented above. After the incubation, each channel was rinsed with a solution of washing buffer. To reduce nonspecific adsorption, a blocking step was performed with the blocking buffer. After a second washing step, each channel was incubated with an about 5 times molar excess of SEB antigens compared to the initially adsorbed anti-SEB Ab amount. After another washing step, the amount of immobilized SEB in each channel was quantified by the adsorption of a 2-fold molar excess of radioiodinated Rb anti-SEB Ab. The channels were then placed in the γ counter, following the procedure already described. Assuming parity between the antibody and the antigen, the bioactivity of the adsorbed antibodies could be calculated for each channel. Background γ counts are corrected using a blank experiment in which radiolabeled antibody was adsorbed in a channel without antigen. All data were corrected using such background correction.

The kinetic studies of immunosorption in the microchannel were performed by first adsorbing about 2 μ L of 3.12 nM Rb anti-SEB Ab for about 1 h in different microchannels. After washing and blocking steps, about 2.1 μ L of 36 nM SEB was added to the microchannel and adsorbed during different times from 1 to 60 min. The adsorbed SEB amount was then revealed by the adsorption of 1 μ L of 0.2 μ M radiolabeled Rb anti-SEB Ab during an incubation time of 1 h. The radioactivity of each channel is then quantified using the γ counter, as already described.

Safety Considerations. All radioactive materials can be hazardous if they are not handled with recommended care. Precautions were taken during the physical handling of radioisotopes, by using disposable latex gloves and operating in a hood equipped with an absolute filter. The prescribed radioactive waste treatment plan was adhered to according to the safety rules of the Radiation Safety Service (RSS).

Results and Discussion

Microchannel Characterization. Laser-treated PET exhibits an increased roughness with respect to native PET as shown in Figure 2a. The surface state of PET after the photoablation has already been studied with atomic force microscopy and confocal Raman spectroscopy in a previous report.²⁰ Generally, the surfaces of the laser-ablated polymers exhibit a larger roughness, and this enhances the surface area. Microscopic inhomogeneities of the surface chemistry after the ablation procedure are

obtained and are probably related to the redeposition of ablated debris. Despite the presence of carboxylic acid groups on the surface,²⁴ the surface oxygen-to-carbon ratio (O/C) generally decreased during the ablation,²⁵ leading to a surface with hydrophobic zones.²⁰ The laminating polymer, which is not laser treated, is smooth as shown in Figure 2b. This layer allows the complete low-temperature sealing of the structure. The surface oxidation of the polyethylene exposed to the channel has been observed by ATR-FTIR spectroscopy and is shown in Figure 2c. The lower spectrum corresponds to the polyethylene surface used in this work, whereas the upper curve represents standard polyethylene. The polyethylene characteristic bands are present in both polymers: the peaks at 2800–3000 cm^{-1} correspond to CH stretch, while those at 1462 and 720 cm^{-1} correspond to CH_2 deformation.²⁶ In the lower spectrum, the band at 1734 cm^{-1} reveals the presence of a C=O stretch, and this is confirmed by the presence of C–O bands in the fingerprint region, as is the case, for example, in PET.²⁶ These bands clearly identify the oxidized layer of the polyethylene surface.

Radiolabeling. The radiolabeling of the proteins was achieved with ^{125}I in order to provide γ -radiation that can penetrate the plastic substrates used in these experiments. The study of protein adsorption in the microchannel devices involving very small volumes requires a very high labeling efficiency of the antibody molecules. The Bolton Hunter reagent²⁷ provided only 250 μCi per 0.25 mL from a 2000 Ci/mmol source, with the result that roughly only one antibody molecule out of 50 000 could be labeled with this reagent. This proved to provide an insufficient signal for adsorption measurements. Therefore, to improve the labeling efficiency, the Markwell procedure²¹ described above was used. It was calculated from the fact that 78.1 pmol of labeled anti-SEB Ab corresponds to about 2×10^6 cpm. Such a rigorous treatment with a radiolabel can affect the specific biological activity of the antibody molecules. To study this effect, the avidity of the anti-SEB Ab before and after the radiolabeling procedure was determined and reported in Figure 3. Before the labeling experiment, the avidity of the antibody for the immobilized SEB is expressed by an apparent K_f of $9.0 \times 10^8 \text{ M}^{-1}$, whereas it is only 10^8 M^{-1} when labeled. This observation shows that the biological activity of radiolabeled antibodies is about an order of magnitude lower than that of the corresponding nonlabeled proteins.

Background and Theory. The specific binding reaction between an antibody (Ab) and an antigen (Ag) is usually driven by electrostatic forces between oppositely charged amino acids, hydrogen bonding, and hydrophobic interactions. This equilibrium reaction, termed "biospecific interaction", is characterized by the affinity of the reactants to form the Ag–Ab complex. The thermodynamic formation constant indicating the strength of such complexes, K_f , can thus be defined as

$$K_f = k_f/k_b \quad (1)$$

where k_f is the kinetic "on rate" for the forward reaction and k_b is the "off rate" for the reverse reaction. Polyclonal antibodies have apparent K_f values between 10^6 and 10^{10} M^{-1} when reacting with different antigens. The kinetics of heterogeneous immunosorption reactions on planar

(18) King, K. D.; Anderson, G. P.; Bullock, K. E.; Regina, M. J.; Saaski, E. W.; Liger, F. S. *Biosens. Bioelectron.* **1999**, *14*, 163–170.

(19) Roberts, M. A.; Rossier, J. S.; Berclier, P.; Girault, H. H. *Anal. Chem.* **1997**, *69*, 2035–2042.

(20) Rossier, J. S.; Berclier, P.; Schwarz, A.; Lorient, S.; Girault, H. H. *Langmuir* **1999**, *15*, 5173–5178.

(21) Markwell, M. A. K. *Anal. Biochem.* **1982**, *125*, 427–432.

(22) Stenberg, M.; Nygren, H. *J. Theor. Biol.* **1985**, *113*, 589–597.

(23) Stenberg, M.; Nygren, H. *J. Immunol. Methods* **1988**, *113*, 3–15.

(24) Lazare, S.; Hoh, P. D.; Baker, J. M.; Srinivasan, R. *J. Am. Chem. Soc.* **1985**, *106*, 4288–4290.

(25) Lazare, S.; Srinivasan, R. *J. Phys. Chem.* **1986**, *90*, 2124–2131.

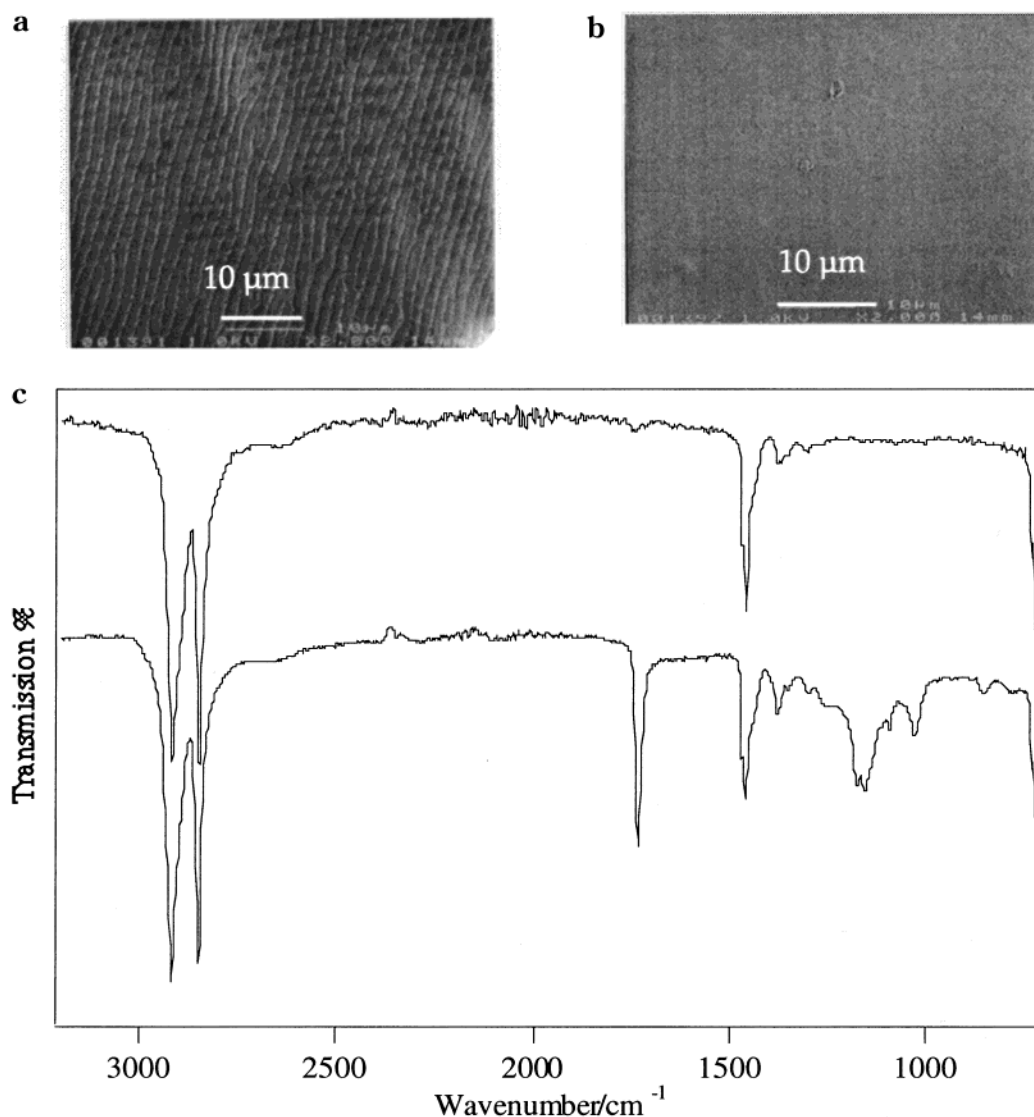


Figure 2. (a) SEM picture of a photoablated PET surface. (b) SEM picture of a non-photoablated PE/PET laminate. (c) ATR-FTIR measurement of the PE/PET lamination.

surfaces is claimed²² to be diffusion controlled and not reaction rate controlled. Rapid immunoassays²³ can hence be performed using shorter diffusion distances to plane surfaces. The surface dimensions of the polymer microchannel, considered here (Figure 1a) are so drastically reduced that the reactants are typically no more than 20 μm apart. The potentially huge advantage of short diffusion distances in these microchannels can only be realized if the rate-determining step for the immunochemical reaction is diffusion controlled rather than being controlled by the inherent forward reaction rate.

The extent of progress of forward immunocomplex formation on a planar surface is indicated by the surface concentration of the diffusing reactant Γ_A ($\text{pmol}\cdot\text{cm}^{-2}$) given by the expression²³

$$\Gamma_A = \frac{2}{\sqrt{\pi}} c_0 \sqrt{Dt} \quad (2)$$

where D and c_0 are the diffusion coefficient ($\text{m}^2 \text{s}^{-1}$) and solution concentration of the diffusing reactant, respectively, while t is the time period after which the surface reaction is analyzed. To substantiate the diffusion control for the reaction carried out in the microchannel, a comparison of the surface concentration ($\text{pmol}\cdot\text{cm}^{-2}$) of

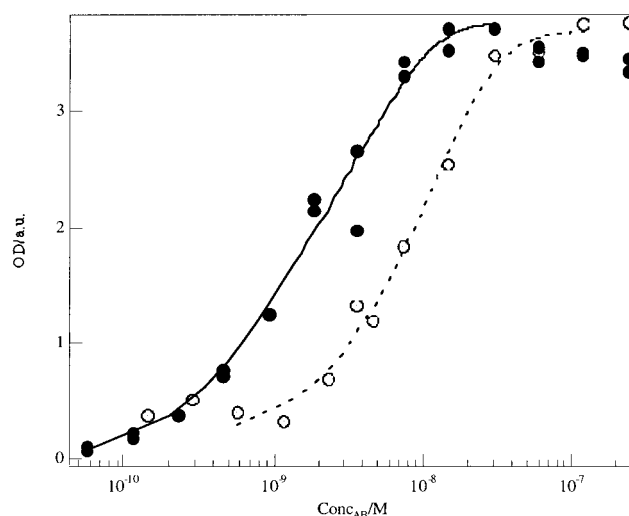


Figure 3. Avidity and apparent K_f measurement of anti-SEB Ab before (closed circles) and after (open circles) the iodination procedure. It can be observed that the isotherm is slightly shifted to the higher concentration, meaning that the avidity of the anti-SEB Ab has been affected by the radiolabeling procedure.

the product formation based on diffusion control (eq 2)

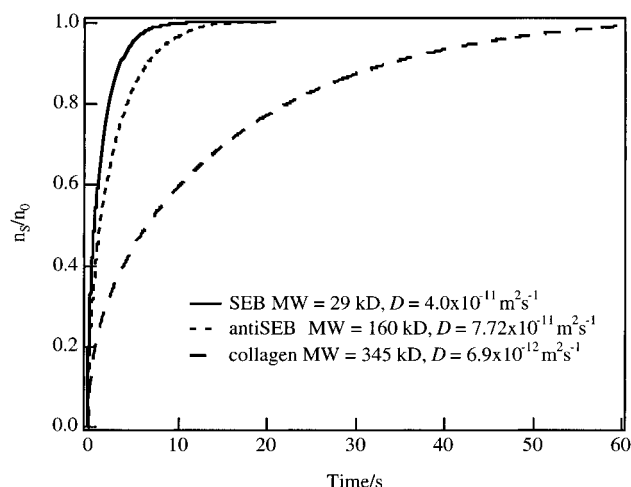


Figure 4. Fick's second-law calculation of the diffusion of molecules reaching the microchannel surface as a function of the incubation time and diffusion coefficient. From the left to the right: SEB (29 kD, $D = 7.72 \times 10^{-11} \text{ m}^2 \text{ s}^{-1}$), anti SEB IgG (160 kD, $D = 4.0 \times 10^{-11} \text{ m}^2 \text{ s}^{-1}$), and collagen (345 kD, $D = 6.9 \times 10^{-12} \text{ m}^2 \text{ s}^{-1}$).

and that obtained from the actual experimental kinetics data (Figure 4) observed in the microchannel is made. The surface concentration, Γ_A , from eq 2, was found using a value of D for an IgG molecule of about $4.0 \times 10^{-11} \text{ m}^2 \text{ s}^{-1}$ with c_0 being $0.2 \mu\text{M}$. Time, t , for both calculations was taken to be 60 s. The diffusion-limited reaction rate on the surface is about $0.016 \text{ pmol} \cdot \text{cm}^{-2} \text{ s}^{-1}$ whereas $0.034 \text{ pmol} \cdot \text{cm}^{-2} \text{ s}^{-1}$ is the rate of product formation on the surface estimated from the experimental kinetics data, thus indicating the reaction's diffusion control. Further, the diffusion distance of a molecule during a given time could be written using a simplified expression

$$L = 2\sqrt{Dt} \quad (3)$$

where L is the diffusion distance (m), t the time (s), and D the diffusion coefficient of a molecule ($\text{m}^2 \text{ s}^{-1}$). It should be noted that D is inversely proportional to the molecular weight of the diffusing molecule, which means that larger proteins need more time to diffuse along a given distance than small ones. Therefore, the diffusion behavior of proteins with different molecular weights was simulated in order to define the limitations of the microdevice. The diffusion of molecules in a fixed volume can be calculated by Fick's second law:

$$\frac{\partial c}{\partial t} + \text{div}(-D \text{grad } c) = 0 \quad (4)$$

where c is the concentration of molecules in the microchannel. This equation expresses the concentration of the molecules that reach the microchannel surface in a given time only by diffusion. In the present case, the fixed volume consists of a rectangular microchannel which is $40 \times 100 \mu\text{m}^2$ in cross section and 2 cm in length. As the third dimension is much longer than the other two, the calculation can be performed in two dimensions.¹¹ The boundary conditions are

$$\text{at } t = 0, c = c_0$$

$$\text{at } t > 0, c = 0 \text{ at the walls}$$

$c = 0$ at the walls because c is the concentration of molecules that are captured once they reach the wall and therefore disappear from the solution.

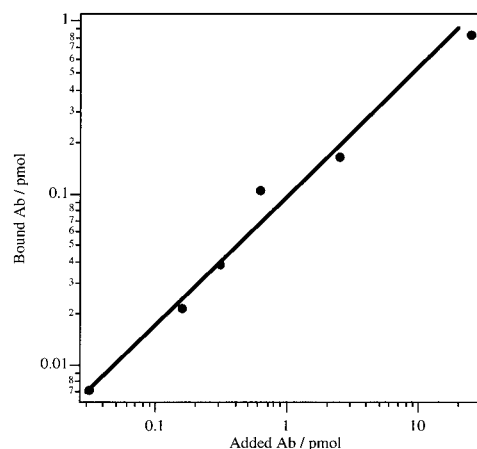


Figure 5. Adsorption isotherm of anti-SEB IgG in photoablated microchannels (2.5 to $2500 \mu\text{g} \cdot \text{mL}^{-1}$ protein solutions were filled in the channel during 1 h of adsorption duration in a wet chamber).

A transient linear algorithm is employed for determining the concentration profile. The simulations are run using commercial finite element software, Flux Expert (Simulog, France), which operates on a Unix workstation (Silicon Graphics Indigo 2 Solid Impact 10000 with 640 Mb RAM).

Numerical Simulation. The ratio n_s/n_0 representing the number of molecules that have reached the microchannel wall versus the total molecules in the channel at $t = 0$ is presented in Figure 4. For this calculation using Fick's second law (eq 4), two different cases are considered. The diffusion of the SEB and anti-SEB IgG which have diffusion coefficients of $7.72 \times 10^{-11} \text{ m}^2 \text{ s}^{-1}$ and $4 \times 10^{-11} \text{ m}^2 \text{ s}^{-1}$,^{15,23} respectively, is considered. This calculation shows that, after 5 s, nearly 100% of the SEB molecules would have reached the surface. The simulation of diffusion of anti-SEB Ab molecules predicts that, after about 15 s, all such molecules would have reached the microchannel surface. A similar calculation for much larger proteins such as collagen (345 kD) having a diffusion coefficient of $6.9 \times 10^{-12} \text{ m}^2 \text{ s}^{-1}$ shows that even such large molecules would need only about 1 min for efficient mass transport to the walls of the microchannel. It is significant to note that, during the adsorption procedure that requires less than 1 s, the microchannel is filled also by forced convection. This should hasten the mass transport toward the wall little more and therefore reduce the time needed by the molecules to reach the surface further. As already explained by eq 1, once the molecule reaches the surface, the reaction with the immobilized antibody is inherently rapid.

Physisorption of the Antibodies. The adsorption of the anti-SEB antibody on the microchannel surface measured by radioactivity is shown in the plot presented in Figure 5. A correlation between the increasing amount of antibody in the channel and the number of adsorbed molecules is clearly evident. Saturation is reached at about 0.81 pmol per channel. As the apparent surface area of the microchannel is about 0.062 cm^2 , this value corresponds to about $13.0 \text{ pmol} \cdot \text{cm}^{-2}$. The saturation value seems reasonable in comparison to $0.5 \text{ pmol} \cdot \text{cm}^{-2}$ obtained on polystyrene microtiter plates and reported literature on other surfaces.²⁸ It is also significant to note that the

(26) Willis, H. A. In *Proceedings of the 5th European Symposium on Polymer Spectroscopy*; Hummel, D. O., Ed.; Verlag Chemie: Weinheim, 1979; p 15.

(27) Bolton, A. E.; Hunter, W. M. *Biochem. J.* **1973**, *133*, 529–539.

(28) Nygren, H.; Werthen, M.; Stenberg, M. *J. Immunol. Methods* **1987**, *101*, 63–67.

volume density of the adsorbed antibodies is quite high, especially considering the maximum adsorption capacity of the microchannel. Indeed, the surface-to-volume ratio of the present system is about 100 times higher than that of a standard microwell.

As already presented, the microchannel is composed of two different polymers, namely the laser-treated PET and the PET/polyethylene sealing lamination layer. It is interesting to compare the amounts of antibody adsorbed on these different polymers. For this purpose, the sealing laminate is peeled off after the incubation and radioactivity on both the laminate, that comprises the "roof" of the channel, and the PET substrate are independently measured. The surface capacities for antibody adsorption are about 5.5 and 19.4 pmol·cm⁻² for the polyethylene lamination and the PET substrate, respectively. The relatively low adsorption of molecules on the laminate is not surprising considering the surface state of the polyethylene. It has been shown in Figure 2c that the polyethylene surface is strongly oxidized. It is usually assumed that an oxidized aliphatic polymer will have a lower affinity for protein adsorption due to its hydrophilicity. For example, poly(ethylene glycol) or poly(ethylene oxide) is commonly used as hydrophilic layers for both immunoassay and implantable devices with low affinity for major proteins.^{29,30} However, antibody adsorption on a laser-treated PET surface, 13.0 pmol·cm⁻² (about 2 μg·cm⁻²), is very much higher than that on the polystyrene (0.5 pmol·cm⁻²) used for our avidity determination study. The present observation is consistent with the results of BSA adsorption on photoablated surfaces, where the authors have found an adsorption 2 to 3 times higher than that on the non-laser-treated plastic.¹³ The reason for this higher protein adsorption is thought to be mainly due to the higher surface area of the laser-treated polymer, as shown in Figure 2a, and the presence of hydrophobic patches on the photoablated PET surface, as seen in the decreased surface O/C ratio, consequent to the laser treatment even though some electrostatic interaction between the protein and the charged photoablated surface cannot be definitively excluded.

Immunosorption Experiments. The bioactivity of the adsorbed antibodies was also measured for different amounts of antibody immobilized per channel, from 0.06 to 0.31 pmol. Despite some aberrant results at lower levels, mainly due to nonspecific adsorption, the mean specific biological activity of the adsorbed antibodies in the microchannel is 30 ± 5%. This amount is not unusual when compared to the literature values.^{31,32}

As already explained, the decrease in assay time is a significant reason for developing microchannel-based immunochemical systems. Therefore, the investigation of the equilibration kinetics³³ is of major interest. The diffusion limitation for the immunochemical surfaces on

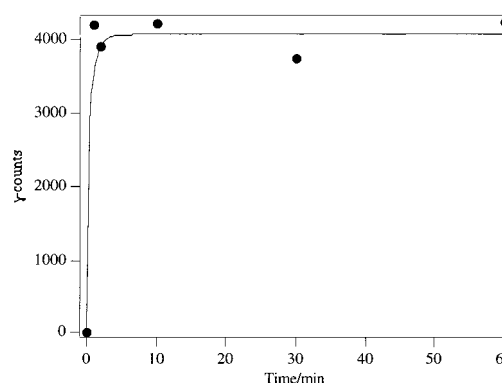


Figure 6. Adsorption kinetics of SEB in the photoablated microchannel. The channel was incubated with 3.12 nM of anti-SEB for 1 h whereas the solution of SEB was incubated at 36 nM between 1 and 60 min and revealed by the secondary radiolabeled anti-SEB at 200 nM.

planar surfaces is usually claimed, which could be calculated in the present case. The rate of the diffusion-controlled forward reaction, from calculations, is found to be about two times lower than the observed rate of the forward reaction on the surface. Also, the effect of incubation time on the immunosorption is presented in Figure 6. It is obvious that the signals detected at increasing incubation times of more than 1 min are not significantly different. Furthermore, it must be pointed out that the kinetics of immunosorption is also enhanced by the forced convection induced during the filling of the channels. This fact along with the high mass transport efficiency in microchannels reduces the incubation time for immunoassays involving reactants of reasonably high affinity to about 1 min.

Conclusion

This report presents results on protein adsorption and immunosorption kinetics in a photoablated PET microchannel. The principal gains offered by this technique are enhanced protein adsorption, increased mass transport efficiency of immunoreactants, and consequent reduction in the equilibration time of the immunochemical reactions. After radiolabeling of the Rb anti-SEB Ab, the physisorption of the polyclonal antibody on the walls of the microchannel was measured and related to the properties of the polymer used for the microfabrication. The bioactivity of the adsorbed antibody, as measured in a sandwich assay, was found to be about 30%. The immunoassay kinetics is in good agreement with numerical simulations of protein transport mainly governed by diffusion control. This report opens the way to the development of a μ-TAS device for immunosorbent assays with either fluorescence or electrochemical detection.

Acknowledgment. The authors would like to thank Alexandra Schwarz, Rosaria Ferrigno, and Valérie Devaud from the Laboratoire d'Electrochimie of the EPFL for helpful discussions and technical support. The help and coordination of the Radiation Safety Service (RSS) at the University of Kansas are also acknowledged. One of us (J.S.R.) wishes to thank the University of Kansas for a visiting fellowship.

LA0006667

(29) Sofia, S. J.; Premnath, V.; Merrill, E. W. *Langmuir* **1998**, *31* (15), 5059–5070.

(30) McPherson, T.; Kidane, A.; Szleifer, I.; Park, K. *Langmuir* **1998**, *14*, 176–186.

(31) Gunaratna, P. C.; Wilson, G. S. *Biotechnol. Prog.* **1992**, *8*, 268–274.

(32) Wimalasena, R. L.; Wilson, G. S. *J. Chromatogr. Biomed. Appl.* **1991**, *572*, 85–102.

(33) Sportsman, J. R.; Liddl, J. D.; Wilson, G. S. *Anal. Chem.* **1983**, *56*, 771–775.